^{13}C CP–MAS NMR Study of Absorbed Water in Polyimide Film

J. F. WATERS,[1] W. R. LIKAVEC,[2] and W. M. RITCHEY[2,*]

[1]Day-glo Color Corp., 4515 St Clair Ave., Cleveland, Ohio 44106, and [2]Department of Chemistry, Case Western Reserve University, Cleveland, Ohio 44106

SYNOPSIS

Solid-state nuclear magnetic resonance (NMR) relaxation studies were performed on Kapton H polyimide films in order to determine the location of water absorption within the polymer lattice and its effects on the microdomain properties of the polymer. Carbon spin lattice relaxation ($^{13}CT_1$), spin lattice relaxation in the rotating frame ($T_{1\rho}$), and inversion recovery cross polarization (IRCP) experiments were performed to analyze wet and dry Kapton films and films exposed to D_2O. The conventional pulse sequences for these experiments were modified with a TOSS acquisition sequence in order to remove spinning side bands from the ^{13}C-NMR spectra. The data indicates that the water molecules aggregate near the carbonyl group of the imide ring and are most probably bound via hydrogen bonding. Additionally the water molecules plasticize the polymer network by increasing the amplitude of low-frequency motions. © 1994 John Wiley & Sons, Inc.

INTRODUCTION

The presence of water in Kapton film has been explored by several workers.[1,2] Results indicate that water tends to bind in two different sites in Kapton film, with one site consistent with singly adsorbed water molecules and another site showing water clusters. The specific chemical sites of water aggregation along the polymer backbone were not determined, however. Deuterium nuclear magnetic resonance (NMR) experiments on D_2O absorbed in Kapton film indicate a molecular reorientation time of approximately 3.5 ns at 200 K for the absorbed water according to measured spin lattice relaxation times (T_1). Thus the water molecules undergo very rapid motions within the polymer lattice, but at the same time seem to occupy specific sites within that lattice. However, correlation times were not determined for both sites in the NMR experiments. Two specific correlation times should have been observed for the different sites assuming different mobilities for the bound versus free molecules.

In order to experimentally determine the chemical sites where the bound H_2O molecules tend to accumulate in rigid polyimides, one must undertake an experimental method that is site specific in its measurements. One such technique is ^{13}C-NMR. Each individual carbon peak may be observed independently, and relaxation measurements can represent what is occurring in the immediately surrounding environment. NMR relaxation measurements such as T_1, spin lattice relaxation in the rotating frame ($T_{1\rho}$), and cross polarization times (T_{CH}) are all determined by an r^{-6} dependence on the motional parameters in the lattice.[3–7] Any residual effects on these motional parameters due to the absorbed water may be investigated via NMR relaxation studies.

EXPERIMENTAL

Instrumentation and NMR Relaxation Measurements

All ^{13}C CP-T_1 experiments were performed on a Bruker AM 300 spectrometer using a magic angle spinning speed of 4500 Hz, a spin lock field of 40

* To whom correspondence should be addressed.

Journal of Applied Polymer Science, Vol. 53, 59–70 (1994)
 CCC 0021-8995/94/010059-12

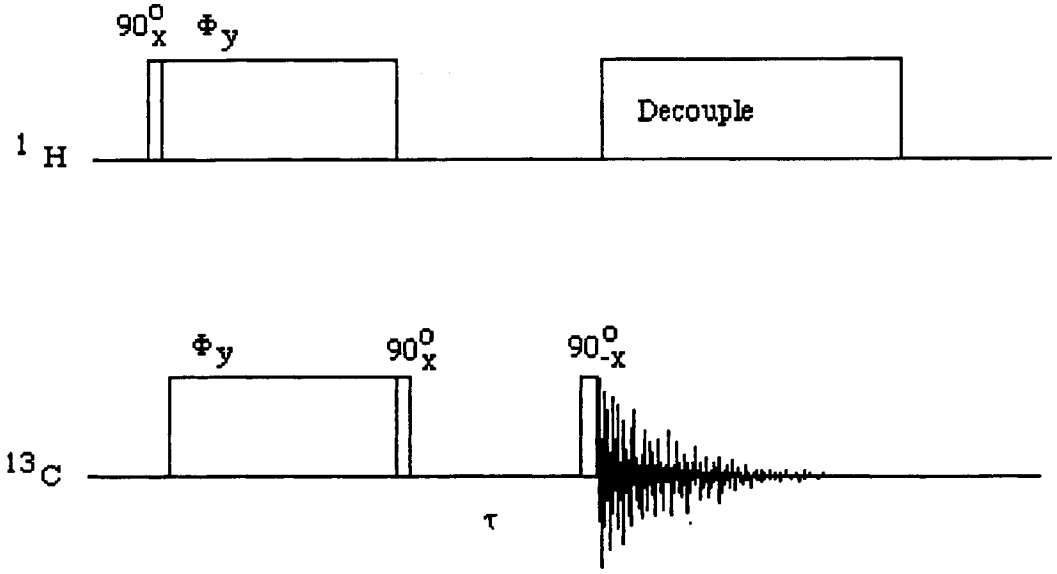

Figure 1 Cross polarization T_1 simulated 180–τ–90 pulse sequence.

kHz, and a pulse sequence as shown in Figure 1. All $^{13}C T_{1\rho}$, $^{1}H T_{1\rho}$, and cross polarization (CP) experiments were conducted on a Bruker MSL 400 spectrometer using a magic angle spinning (MAS) speed of 3500 Hz and total suppression of spinning sidebands (TOSS) acquisition since spinning sidebands could not be removed from the region of interest on the 400-MHz instrument by MAS. Pulse sequences for $^{13}C T_{1\rho}$ and $^{1}H T_{1\rho}$ measurements are shown in Figures 2 and 3, respectively. Cross polarization time (T_{CH}) measurements were measured using a modified inversion-recovery cross polarization pulse sequence combined with TOSS acquisition. The pulse sequence is shown in Figure 4.

Materials

Kapton H film of 50 μm thickness was purchased from DuPont Chemical and was vacuum dried at 120°C overnight prior to use. Deuterium oxide was purchased from Cambridge Isotope Labs and used as received. Water was double distilled prior to use.

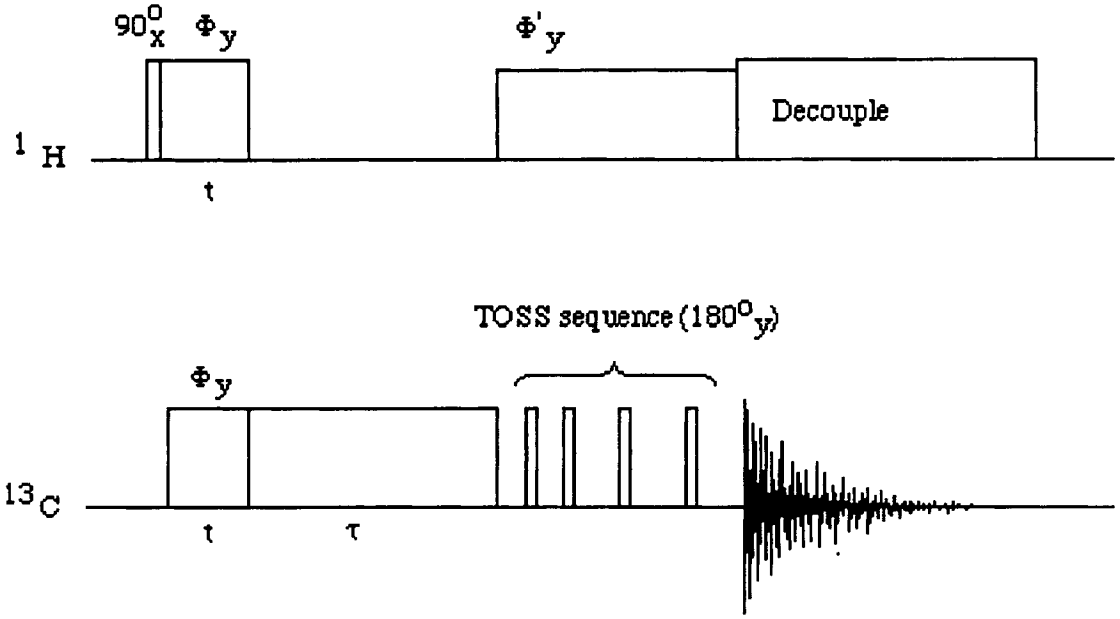

Figure 2 Combined ^{13}C $T_{1\rho}$/TOSS pulse sequence.

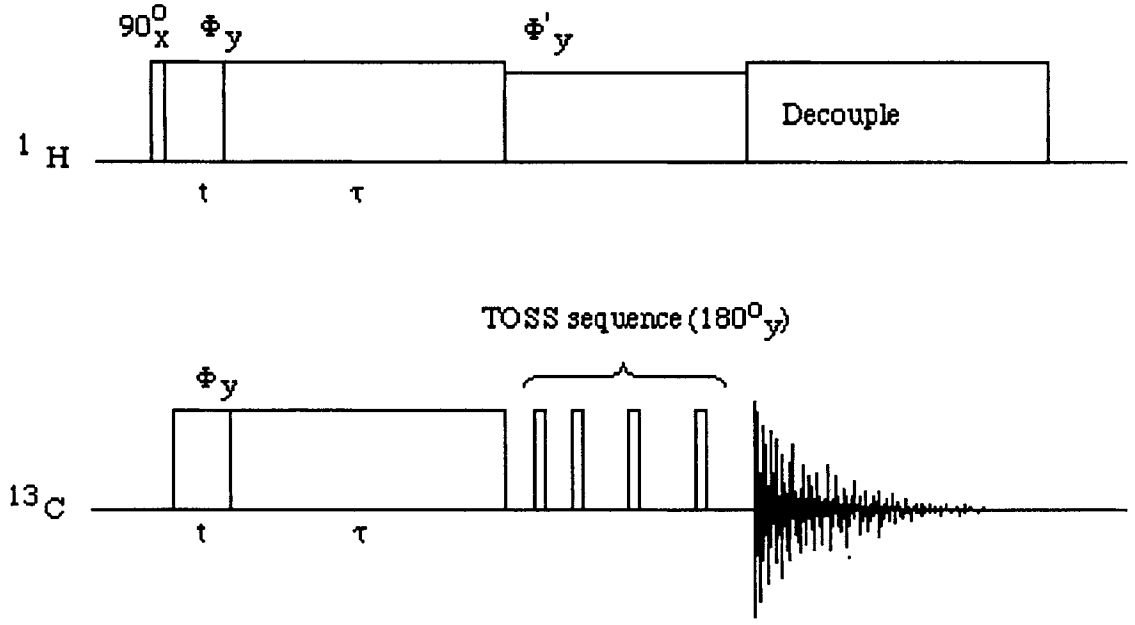

Figure 3 Combined ^1H $T_{1\rho}$/TOSS pulse sequence.

RESULTS AND DISCUSSION

CP–MAS Spectrum of Kapton Film

The CP–MAS spectrum of Kapton film spun at 4500 Hz in a 7.05-Tesla magnetic field (300 MHz proton resonance) is shown in Figure 5. The structure of Kapton H film is shown in Figure 6, and the peak assignments are given in Table I.[8] Three nonoverlapping resonances are observed: the carbonyl peak at 165 ppm, the oxygen-substituted aromatic peak at 156 ppm, and the carbonyl-substituted aromatic peak at 137 ppm. All other aromatic resonances, although observable, overlap to various degrees, and deconvolution of the relaxation data to quantify results is not possible. However, good qualitative data may still be obtained from the relaxation measurements.

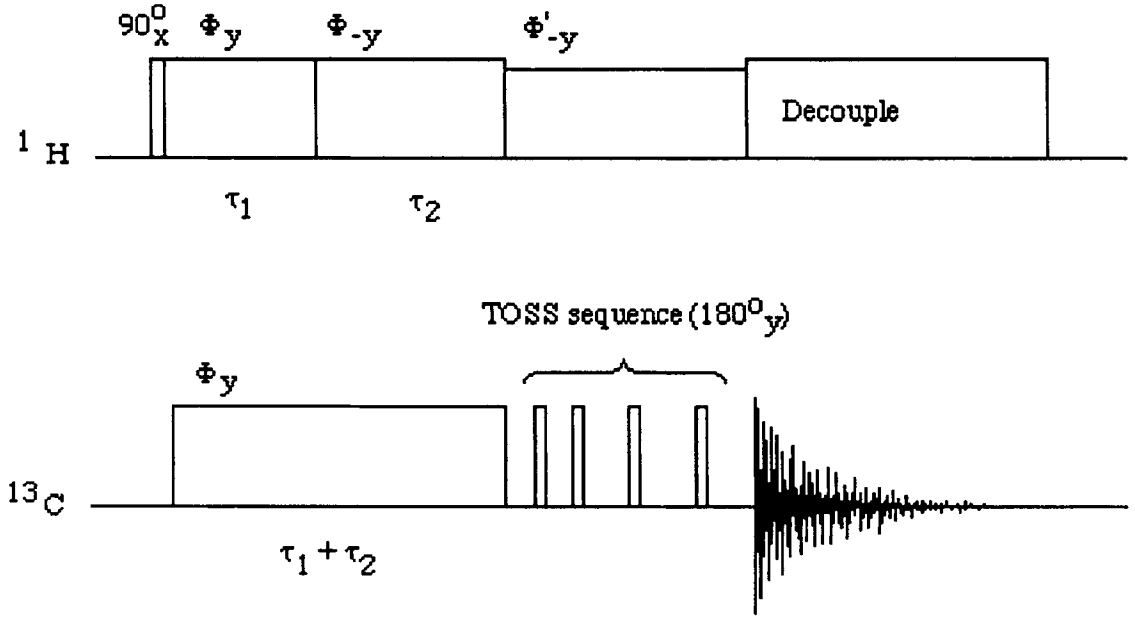

Figure 4 Combined IRCP T_{CH}/TOSS pulse sequence.

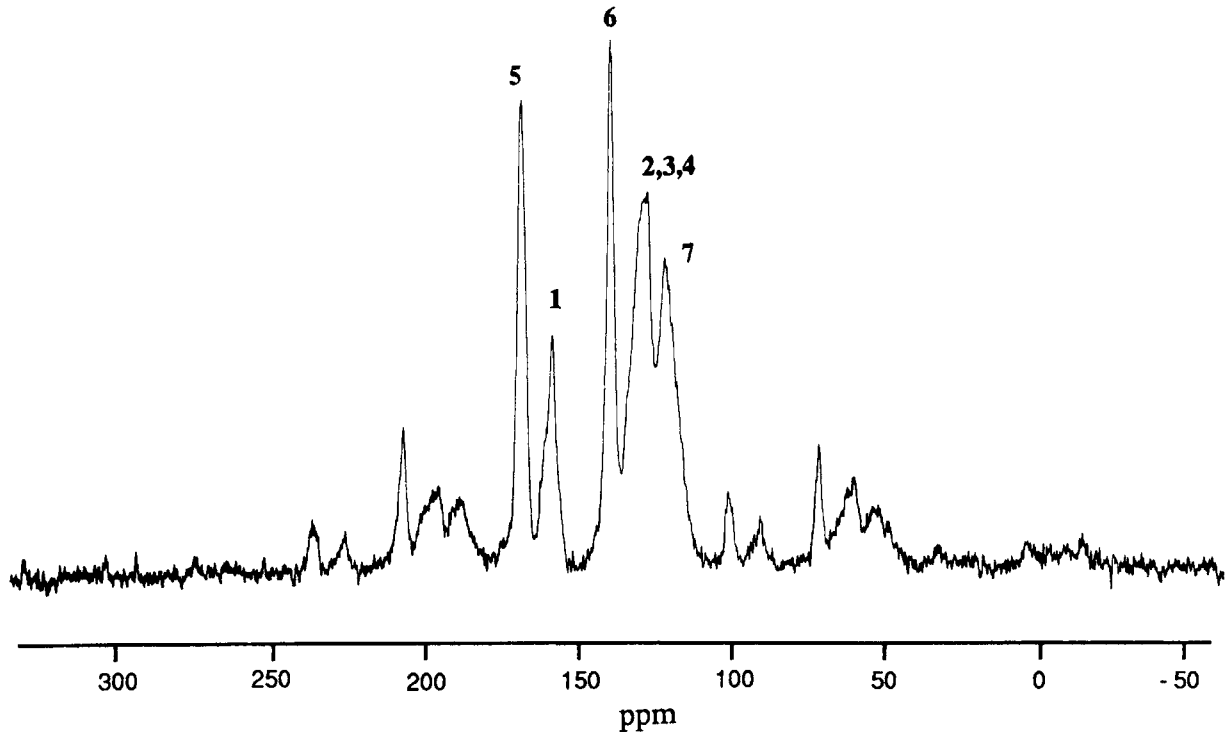

Figure 5 75.4-MHz ^{13}C CP–MAS spectrum of Kapton H film spun at 4500 Hz.

T_1 Measurements of Kapton Film

The T_1 relaxations of dried Kapton polyimide film, the same sample containing 3.1% absorbed H_2O and 3.2% D_2O are shown for the 165- and 125-ppm resonances in Figures 7 and 8, respectively. The relaxation decays for all resonances were fit to Eq. (1):

$$M(t) = M_0[X \exp(-t/T_{1A}) + (1 - X)\exp(-t/T_{1B})] \quad (1)$$

where $M(t)$ is the magnetization at time t, M_0 is the initial magnetization, X and $(1 - X)$ are the two components of the decay that relax with time constants T_{1A} and T_{1B}. The values for X, T_{1A}, T_{1B}, the χ^2 fitting parameter, and the weighted average mean $\langle T_1 \rangle$ are given in Table II.

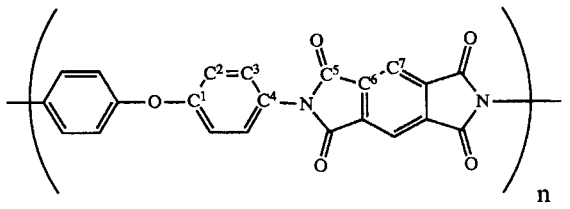

Figure 6 Structure of Kapton H polyimide film.

An obvious increase in the mean T_1 relaxation rate $\langle T_1 \rangle$ is observed for both the D_2O and the H_2O absorbed film in the 165- and 137-ppm carbons, while the other peaks do not show significant changes from wet to dry. In addition, the D_2O and the H_2O absorbed film show similar relaxation rates. Several studies on effects of absorbed water in polyimides show a decrease in glass transition temperature of the polymer from moisture absorption, suggesting plasticization.[9,10] Because T_1 is dependent on molecular motion in the MHz range, plasticization of the polymer at room temperature would be evident by a change in the T_1 relaxation rate. This

Table I Chemical Shifts of In Kapton H Polyimide Film

Carbon	ppm
C^1	156
C^2	127[a]
C^3	125[a]
C^4	132[a]
C^5	165
C^6	137
C^7	120

[a] Overlapping resonances.

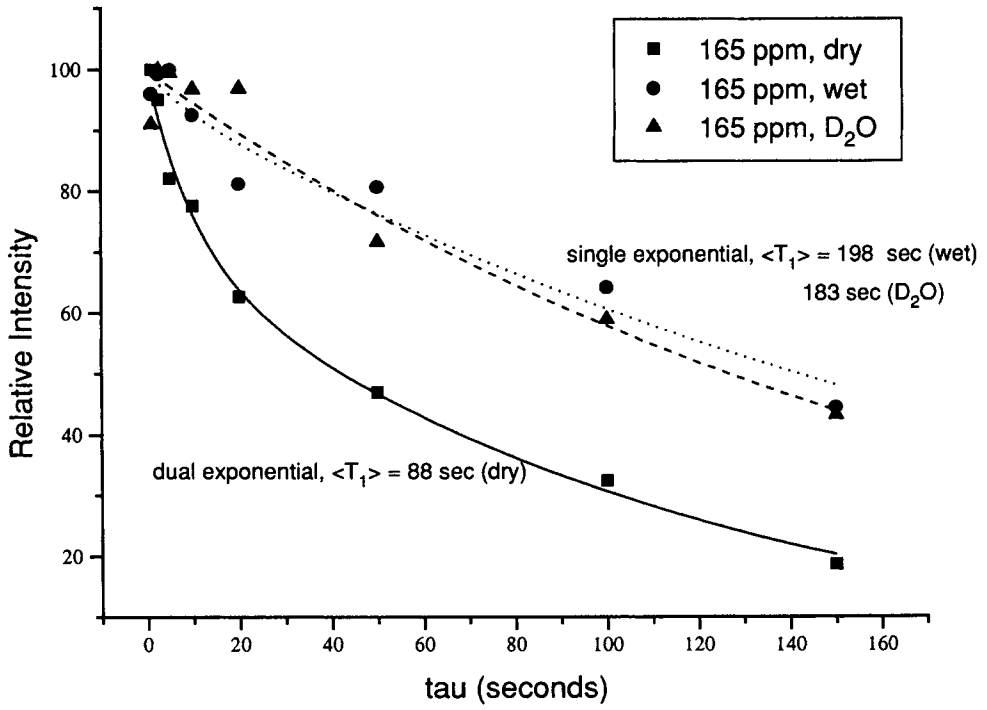

Figure 7 ^{13}C T_1 decay of 165-ppm carbon in Kapton H polyimide film.

is what is observed for the 165- and 137-ppm resonances. However, while these carbon resonances show significant changes in the relaxation rate, others show virtually no change at all. Furthermore, if plasticization were occurring in the polymer, even in submicron domains,[11] one would expect to observe changes in the T_1's for each peak in the spectrum. What is observed, however, is that only the 165- and

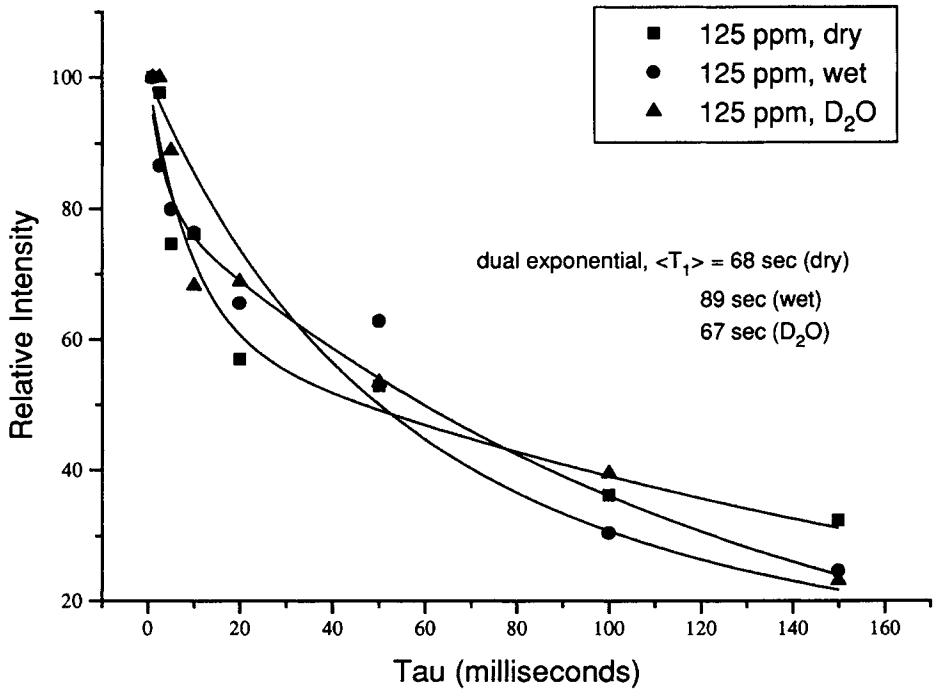

Figure 8 ^{13}C T_1 decay of 125-ppm carbon in Kapton H polyimide film.

Table II Carbon[13] T_1 Values in Kapton H Dry, H_2O Absorbed, and D_2O Absorbed Films

Resonance (ppm)	X	T_{1A} (s)	T_{1B} (s)	$\langle T_1 \rangle$ (s)	χ^2
165 dry	0.294	10.2	120	88	0.086
165 wet	—	—	198	198	0.20
165 D_2O	—	—	183	183	0.23
156 dry	0.39	9.46	221	139	0.38
156 wet	0.19	3.31	123	103	0.32
156 D_2O	0.24	7.86	139	107	0.36
137 dry	0.39	17.0	153	100	0.19
137 wet	—	—	163	163	0.35
137 D_2O	—	—	151	151	0.12
125 dry	0.56	13.0	138	68	0.37
125 wet	0.33	7.20	131	89	0.23
125 D_2O	0.30	13.0	89.5	67	0.06
120 dry	0.18	4.77	68.0	56	0.26
120 wet	0.52	11.2	153	79	0.11
120 D_2O	0.48	11.9	120	66	0.18

137-ppm carbons show significant changes in the T_1 from wet to dry. On the basis of these arguments, changes in polymer motion in the MHz range due to moisture are ruled out as contributing to changes in the T_1's of the 165- and 137-ppm resonances in Kapton.

This leaves two possibilities that may explain the increase in the T_1 of the 165- and 137-ppm carbons in the moisture-absorbed polymer. These are either dipolar relaxations due to translational motions of paramagnetic oxygen or some other magnetically active species, or changes in T_1 relaxations via changes in the chemical shift anisotropy (CSA) shielding parameters due to absorbed water.

CSA contributions to T_1 in chemical species are recognizable by both multiple exponential decay of each resonance as well as pronounced differences in the relaxation rates from peak to peak depending on differences in CSA shielding parameters,[12] depending on the square of the anisotropies of each carbon. CSA contributions to T_1 are described for axially symmetric species as:

$$1/T_1 = (1/15)\gamma^2 B_0^2(\sigma// - \sigma\perp) \times [2\tau_c/(1 + \omega^2\tau_C^2)] \quad (2)$$

where γ is the gyromagnetic ratio of the nucleus, and $(\sigma// - \sigma\perp)$ is the difference in the shielding factor of the nucleus perpendicular and parallel to the external magnetic field B_0. One may argue that CSA effects according to Eq. (2) require a correlation reorientation time similar to the reorientation time for the dipolar mechanism. However, such a correlation time is provided for under magic angle spinning at 4500 Hz. In Kapton film, all carbons are sp^2 hybridized (either aromatic or carbonyl), and should possess similar CSA shielding parameters,[13] hence should show similar T_1 relaxations. This holds true experimentally, hence CSA cannot be ruled out as a significant contributor to T_1 from the T_1 study alone. The change in the relaxation rates of the 165- and 137-ppm carbons due to changes in the CSA shielding parameters can be ruled out, however, based on the $^{13C}T_{1\rho}$ results discussed in the next section, which show similar trends in the relaxations of dry and moisture-absorbed samples. The $^{13C}T_{1\rho}$ magnetization decays for the 165- and 120-ppm resonances are shown in Figures 9 and 10. Although the same relaxation mechanisms may not be dominating the T_1 and $^{13C}T_{1\rho}$, it appears the same mechanism retarded in T_1 measurements by the presence of water or D_2O is also retarded in the $^{13C}T_{1\rho}$ measurements. According to Eq. (2), the CSA relaxation occurs according to the square of the magnetic field B_0. If changes in the CSA shielding parameters of carbon resonances 165 and 137 ppm due to the presence of absorbed water were causing changes in T_1, one would not expect this same effect to be observed in the low field spin lock $T_{1\rho}$ relaxation. Therefore, although CSA may provide a relaxation mechanism for T_1, this relaxation mechanism is most probably not altered to any significant extent by the presence of absorbed water. This leaves the only plausible explanation to the changes in T_1 from absorbed water to be via changes in the dipolar relaxation mechanism from translating magnetically active species, the most probable candidate being triplet oxygen. Thus, some type of steric exclusion of a translating magnetically active species from the carbonyl carbon must be occurring in the Kapton film.

Some insight into the mobility of the absorbed water molecules can be gained by examining the T_1 relaxations of the H_2O- and the D_2O-absorbed Kapton films. Assuming a close proximity of H_2O to the 165 ppm carbonyl (presumably through hydrogen bonding), and not speculating on any other relaxation mechanisms, a mobile water molecule alone will provide a relaxation pathway through a translational dipolar mechanism. If this were occurring, the D_2O-absorbed Kapton would show a slower T_1 rate based on the square of the gyromagnetic ratios in Eq. (3). Spin lattice relaxation time has been defined for a simple I and S spin system for a single correlation time as:[14]

$$1/T_1 = (2/15)\gamma_I^2\gamma_S^2(h/2\pi)^2 S(S+1)r^{-6}[\tau_c/(1 + (\omega_I - \omega_S)^2\tau_c^2) + 3\tau_c/(1 + \omega_I^2\tau_c^2) + 6\tau_c/(1 + (\omega_I + \omega_S)\tau_c^2)] \quad (3)$$

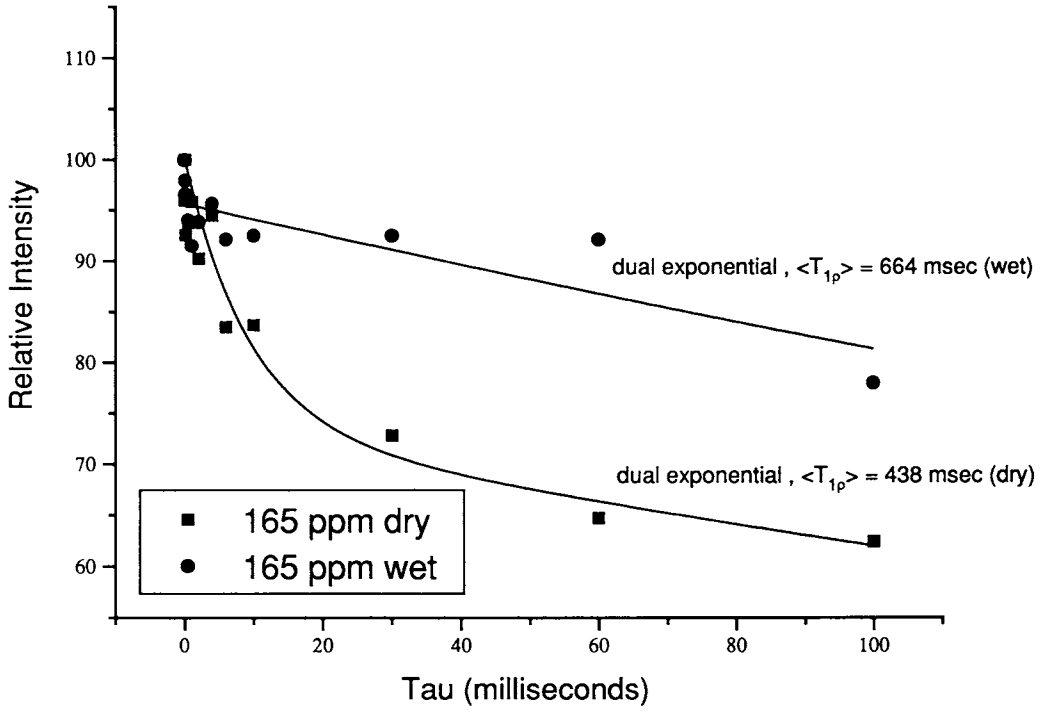

Figure 9 $^{13}C\ T_{1\rho}$ decay of 165-ppm carbon in Kapton H polyimide film.

where γ_I and γ_S are the gyromagnetic ratios of the I and S spins, r is the internuclear distance, ω_I and ω_S are the Larmor frequencies of the I and S nuclei, and τ_c is the molecular reorientation correlation time. Deuterium has a gyromagnetic ratio about 0.154 times that of protons, and the contribution to T_1 by this mechanism in D_2O should be about 1/40th that of H_2O. However, the H_2O- and D_2O-ab-

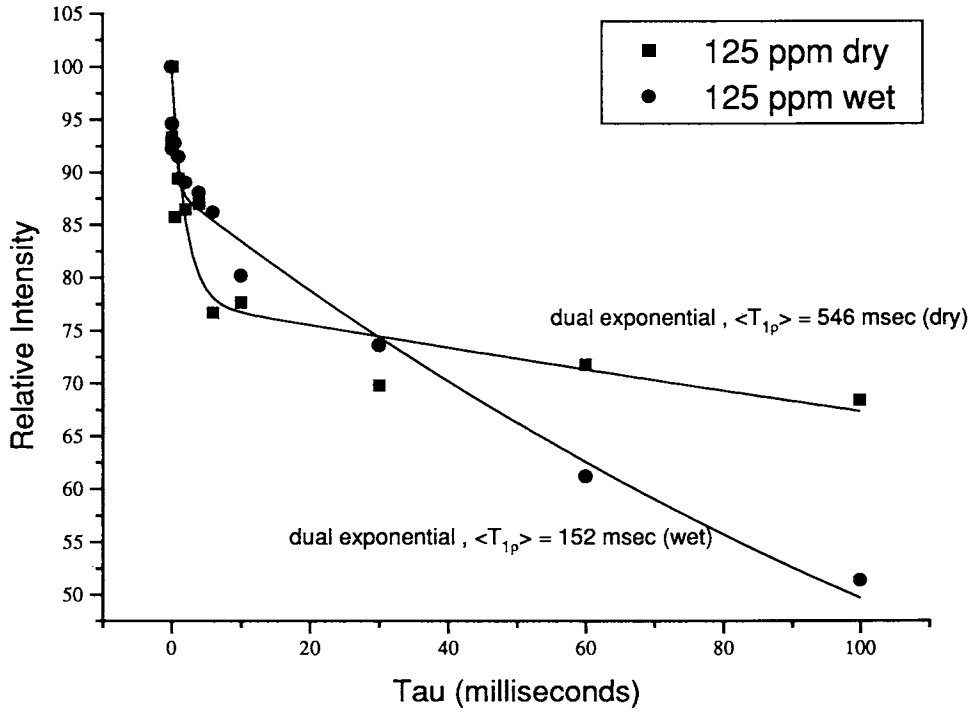

Figure 10 $^{13}C\ T_{1\rho}$ decay of 125-ppm carbon in Kapton H polyimide film.

sorbed films show nearly identical T_1 relaxation rates. Based on this fact, it is obvious that no translation of the water molecule occurs on the MHz time scale. Thus, the water protons remain relatively fixed in the polymer matrix at the carbonyl carbon.

It has been previously suggested that polymers can form charge transfer (or π donating) complexes in the solid state,[15] and that polyimides specifically may form these types of complexes.[15-17] The exact nature of this interaction is not completely understood, but in Kapton alignment should occur in a face-to-face manner through electron-poor imide rings with the relatively electron-rich nitrogen and oxygen-substituted ring of the oxydianiline monomer.[17] In this type of "layered" charge transfer complexation, approach of a translating species cannot occur above or below the plane of the imide ring, and it is obvious that the presence of water hydrogen bonded to the carbonyl within the imide ring plane could significantly prevent the approach of any species to the carbonyl carbon through steric factors. In addition, since the water molecule is relatively less mobile at the carbonyl, this steric effect would be effective for long periods of time on the NMR T_1 time scale, and the effect should be observable by NMR relaxation measurements. If the pathway of translating paramagnetic species were blocked by bound water, one would expect a significant increase in the T_1 relaxation rates of the carbonyl resonance at 165 ppm, but one would also not expect to see an effect in carbons far removed from the presence of the absorbed water. This is exactly what is observed, with the greatest effect seen in the 165- (carbonyl) and 137-ppm (carbonyl-substituted aromatic) carbons, and little effect on the T_1 of any other peaks in the spectrum. However, this does not rule out the presence of water in other areas of the polymer chain, but simply implies that water molecules at other sites remain relatively mobile.

This explanation agrees quite well with the work of Xu et al.[2] who identified the two sites of water molecules in Kapton film by deuterium NMR line shape analysis and dielectric analysis. They found relatively less mobile water molecules in films containing less than 2% absorbed water, and more mobile molecules when the film became saturated (3.1% absorbed water). Thus, it is apparent from our experiments that the less mobile site for bound water at low levels of moisture absorbance is hydrogen bound to the imide carbonyl, but it is impossible to speculate on the nature of the location of the more mobile site. Previous authors have shown that this more mobile site can be explained by aggregation of water molecules in free volume areas within the polymer lattice.[2]

Previous studies on D_2O absorbed in Kapton film gave a correlation time of approximately 3.5 ns for molecular motion at 200 K based on a $^{D}T_1$ minimum.[1] This apparently does not agree with our assessment of the relative immobility of the absorbed water in our Kapton specimen. However, in the $^{D}T_1$ analysis performed, only one component of the $^{D}T_1$ relaxation was accounted for, thus the slower motions of relatively immobile water may not have been taken into account in the analysis. One can only characterize the relative mobility of multiple sites by performing multiple component T_1 analysis of the absorbed water or D_2O directly, thus determining the relative amount and mobility of the multiple sites of water aggregation.

$T_{1\rho}$ and T_{CH} Measurements on Kapton Film

The $^{1H}T_{1\rho}$ measurements for each carbon resonance in dry, D_2O-absorbed, and water-absorbed Kapton film is given in Table III. All the values are similar, not only among each resonance of the three samples but also between resonances within each sample. Additionally, single exponential decay is observed in all cases. This suggests that the main relaxation mechanisms of the protons are occurring through efficient ^1H–^1H spin diffusion,[18] and changes in regional motions will not effect the $^{1H}T_{1\rho}$ to any measurable extent.

The $^{13C}T_{1\rho}$, however, show very different behavior from the $^{1H}T_{1\rho}$ results. Since ^{13}C is a very dilute nucleus, spin diffusion cannot occur to any appreciable extent, and regional differences in relaxation rates can be observed, similar to $^{13C}T_1$ measurements. The measured $^{13C}T_{1\rho}$ relaxations for H_2O-absorbed and dried Kapton film were shown previously in Figures 9 and 10. Two component exponential fits to the data were performed according to Eq. (1), and the results are given in Table IV. $^{13C}T_{1\rho}$ relaxation rates are sensitive to exactly the same types of relaxation mechanisms as are $^{13C}T_1$ relaxation rates. $T_{1\rho}$ relaxations, however, are occurring at very low magnetic field strengths (the

Table III ^1H $T_{1\rho}$ Values in Kapton H Film: Dry, Wet, and D_2O Absorbed

Resonance (ppm)	^1H $T_{1\rho}$ (dry) (ms)	^1H $T_{1\rho}$ (wet) (ms)	^1H $T_{1\rho}$ (D_2O) (ms)
165	12.1	12.1	13.0
156	10.1	10.6	9.1
137	11.4	12.8	10.8
125	9.1	8.1	9.8
120	10.0	9.9	10.0

Table IV Carbon[13] $T_{1\rho}$ in Wet and Dry Kapton H Film

Resonance (ppm)	X	$T_{1\rho}$ (A) (ms)	$T_{1\rho}$ (B) (ms)	$\langle T_{1\rho} \rangle$ (ms)	χ^2
165 dry	0.27	9.55	597	438	0.17
165 wet	0.06	0.062	707	664	0.073
156 dry	0.098	4.90	389	351	0.16
156 wet	0.056	9.47	217	205	0.066
125 dry	0.22	1.96	700	546	0.28
125 wet	0.12	0.54	173	152	0.090
120 dry	0.24	9.72	319	245	0.17
120 wet	0.16	2.20	121	102	0.057

strength of the spin-lock field). Relaxation rates are therefore sensitive to slower motions during dipolar relaxations, with motional sensitivity in the kilohertz range. Because of the very rigid polymer lattice and the lack of molecular motions in Kapton, one would probably expect spin–spin interactions to play a significant role in the $^{13C}T_{1\rho}$ mechanism.[14] Therefore, drawing quantitative conclusions on the relaxation rates based solely on molecular motions should not be attempted. Despite this limitation, we observe a marked increase in the 165-ppm (carbonyl) relaxation rate, while other carbons show a marked decrease in $^{13C}T_{1\rho}$. Unfortunately, the relaxation rate of the 137-ppm carbon could not be determined because this resonance relaxed too slowly for the spin locked times used in the experiment. These observations are consistent with the T_1 study, which showed similar trends. This behavior suggests that the $^{13C}T_{1\rho}$ for the 165-ppm carbon is relaxing to a significant extent by similar mechanisms as the $^{13C}T_1$, most probably via translating paramagnetic species, which is being hindered for the carbonyl by bound water. The observed decrease in the $^{13C}T_{1\rho}$ for the other resonances may be explained by plasticization of the polymer by absorbed water (without taking into account spin–spin interactions). The distribution function of molecular motions in the kilohertz range appears to have increased in the H_2O- and D_2O-absorbed samples, thus the more efficient $^{13C}T_{1\rho}$ relaxation. Therefore plasticization of the polymer can be supported from the $^{13C}T_{1\rho}$ data, but not directly proven until the extent of spin–spin interactions has been determined.[19,20]

Inversion recovery cross polarization measurements of the 165- and 137-ppm resonances in wet and dry Kapton films are shown in Figures 11 and 12, respectively. Two component fits to the cross polarization times were conducted according to Eq. (4):[21]

$$M(t) = M_0 \exp(-t/{}^{H}T_{1\rho}) \times \{(X)[2\exp(-t/T_{CH1}) - 1] + (1 - X)[2\exp(-t/T_{CH2}) - 1]\} \quad (4)$$

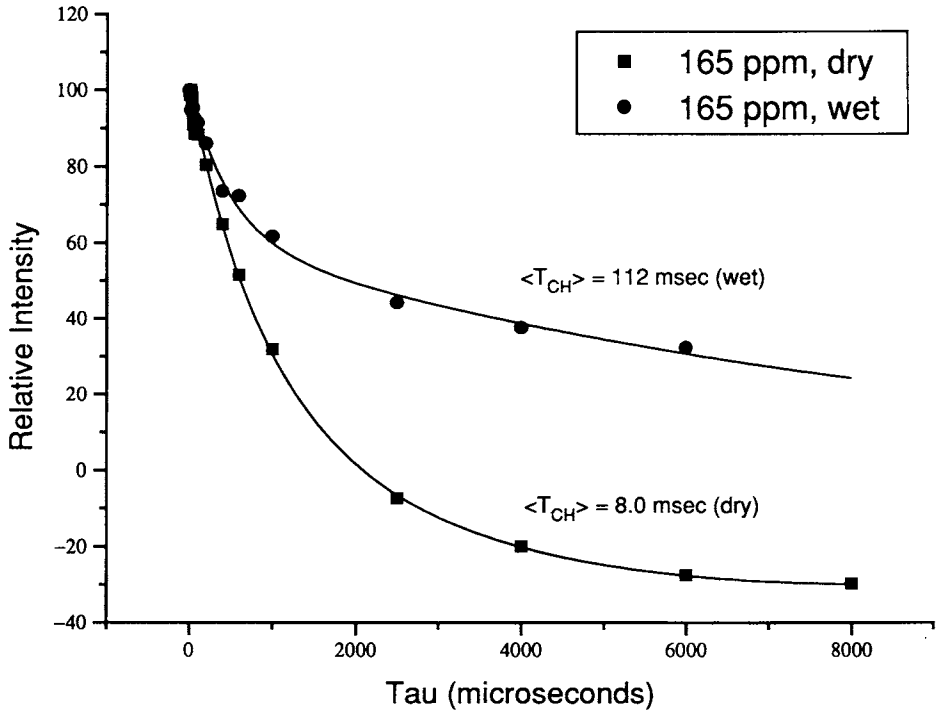

Figure 11 IRCP of 165-ppm carbon resonance in Kapton H polyimide film.

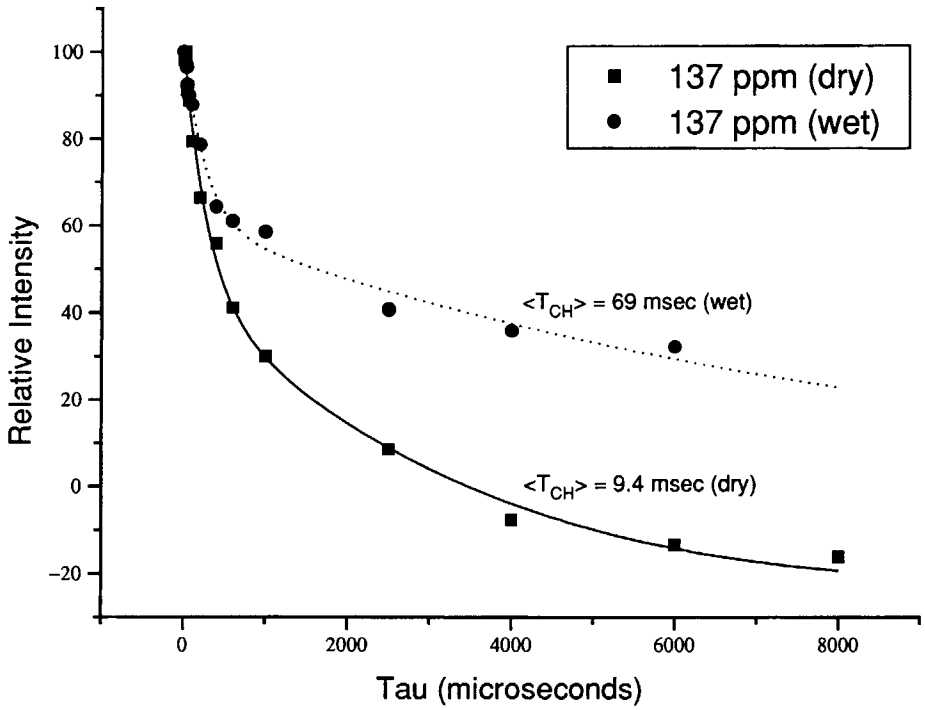

Figure 12 IRCP of 125-ppm carbon resonance in Kapton H polyimide film.

where $M(t)$ is the magnetization at time t, M_0 is the initial magnetization, ${}^{H}T_{1\rho}$ is the proton $T_{1\rho}$, X is the portion of the relaxation curve cross polarizing with a time constant of T_{CH1}, and $(1 - X)$ is the portion of the curve cross polarizing with a time constant of T_{CH2}. The values for X, T_{CH1}, T_{CH2}, the χ values of the fit, and the mean cross polarization value $\langle T_{CH} \rangle$ (the weighted average of each component) are given in Table V. The cross polarization is retarded in all carbons by the presence of the absorbed water molecules, the largest effect is seen in the 165-ppm carbonyl carbon, where the $\langle T_{CH} \rangle$ increased by a factor of 18. The $\langle T_{CH} \rangle$ values in both the carbonyl-substituted and the oxygen-substituted aromatic carbons (137 and 156 ppm, respectively) are both increased by a factor of about 7.5, while the 120- and 125-ppm aromatic carbons are both increased by a factor of about 3.3. Cross polarization occurs according to Eq. (5), with sensitivity toward molecular motions in the near static range, and spatial selectivity based on an r^{-6} dependence on the cross polarization time. The cross polarization depends upon the precision of the Hartmann–Hahn match, the internuclear distance between the cross polarizing nuclei (r), and the extent to which the process is modulated by molecular motion as shown in Eq. (5).

Table V Inversion Recovery Cross Polarization Times (TCH) Values in Kapton H Film: Wet and Dry

Resonance (ppm)	X	T_{CH1} (ms)	T_{CH2} (ms)	$\langle T_{CH} \rangle$ (ms)	χ^2 ($\times 10^{-2}$)
165 dry	0.43	1.06	8.00	5.02	1.07
165 wet	0.20	0.57	112	89.8	1.31
156 dry	0.33	0.14	4.16	2.83	2.90
156 wet	0.36	0.22	32.3	20.7	4.67
137 dry	0.28	0.34	9.44	6.89	2.10
137 wet	0.22	0.32	68.7	53.7	1.77
125 dry	0.33	0.10	4.27	2.89	7.60
125 wet	0.28	0.08	13.2	9.53	4.90
120 dry	0.38	0.033	5.27	3.28	7.81
120 wet	0.48	0.038	21.3	11.1	18.6

$$1/T_{CH} = (\pi^{1/2}/4)(\sin^2\theta_C \sin^2\theta_H M_2^{CH}) \times \{\tau_C \exp[(\Delta\omega^2\tau_C^2)/4]\} \quad (5)$$

where T_{CH} is the cross polarization time constant, θ_C and θ_H are the angles between the external magnetic field and the spin lock fields of the respective nuclei, M_2^{CH} is the second moment of the heteronuclear dipolar coupling interaction, τ_C is the average molecular reorientation time, and $\Delta\omega$ is the angular mismatch of the Hartmann–Hahn condition.

The observations of the extreme increase in cross polarization times with the absorbed water can be explained in motional terms. Two possibilities exist: either the increased concentration of water molecules mobile on the cross polarization time scale or an increase in the motions of the polymer itself on a time scale slow enough to not effect the T_1 of the polymer. The first possibility of water molecules providing a motional parameter whereby the proton reservoir is experiencing a fluctuation with respect to the spin lock field can be ruled out from the $^{1H}T_{1\rho}$ measurements, which are identical in both the wet and dry samples. Significant coupling of the water and polymer protons should cause a faster $^{1H}T_{1\rho}$ in the moisture-absorbed sample through spin diffusion through the motional water molecules.[22] The lack of change in this relaxation time with absorbed water suggests that little magnetic interaction is occurring between the water and the polyimide. Thus we must consider the change in the inversion recovery cross polymerization (IRCP) time to be due to an increase in the motional parameters of the polymer itself, i.e., plasticization of the Kapton by absorbed water. This is consistent with previously investigated polyimide–water interactions, and also agrees with our $^{13C}T_{1\rho}$ measurements.

If an increase in the cross polarization times is attributed to an increase in the motional parameters of the polymer, then one must also explain the extremely large increase in the $\langle T_{CH} \rangle$ of the 165-, 156-, and 137-ppm carbon resonances compared to the 125- and 120-ppm resonances. This large difference in behavior is due to the fact that the 165-, 156-, and 137-ppm resonances are all quaternary carbons. Without attached protons, cross polarization must occur with more distant protons in the polymer chain, thus these resonances are more sensitive to changes in molecular motion and free volume within the polymer lattice. The increase in distance to the cross polarizing nuclei changes the behavior of the cross polarization, and comparing the relative changes in $\langle T_{CH} \rangle$ of protonated and nonprotonated carbons should not be done in a quantitative manner.

CONCLUSIONS AND FURTHER STUDIES

We have identified the regions of bound water in Kapton H film through $^{13C}T_1$, IRCP, and $^{13C}T_{1\rho}$ measurements to be the carbonyl group of the imide ring. The large increase in the observed $^{13C}T_1$ of the 165- and 137-ppm carbon resonances indicates that the water molecules appear to be tightly bound to this group. IRCP results indicate that plasticization of the Kapton H film has occurred in the water-absorbed samples, with significant changes observed for each resonance in the spectrum. The $^{13C}T_{1\rho}$ results support on a qualitative basis the T_1 and IRCP data, and indicate that the plasticization has most likely occurred via an increase in low-frequency molecular motion. The $^{13C}T_{1\rho}$ may be effected to a large extent by spin–spin interactions in polyimides, and it is difficult to assign quantitative motional significance to the changes in these relaxation rates from the data.

^{13}C-NMR CP–MAS measurements, because of their site-specific nature, provide a very powerful tool for assessing the motional effects of water on polyimide systems, as well as the chemical regions of water aggregation. Further studies on the multicomponent T_1 analysis of absorbed D_2O in Kapton film at various temperatures should provide greater insight into the relative amounts and mobility of the various sites of bound water within the polymer lattice. Studies on polyimides with linear aliphatic diamines, which should not tend to form charge transfer complexes in the solid state, should be observed for T_1 relaxations to see if the presence of water inhibits the carbonyl relaxation to the same extent as in Kapton film. The differences in the mechanical behaviors of polyimide films and powders should provide very different NMR behaviors, and an investigation of differences in the NMR relaxation behaviors of polyimide systems with respect to various processing parameters should be of interest to the polyimide industry.

CP–MAS NMR investigations on polyimides are sparse in the literature because of limitations in observation of the solid-state ^{13}C spectrum (spinning sidebands, many overlapping resonances). The combined TOSS–relaxation pulse sequences presented here overcome the limitation of spinning sidebands in virtually all solid-state polyimide NMR spectra. With the successful demonstration of these pulse sequences, further investigations of polyimides via CP–MAS NMR is possible.

REFERENCES

1. S. Z. Li, Y. S. Pak, K. Adamic, S. G. Greenbaum, B. S. Lim, G. Xu, and A. S. Norwick, *J. Electrochem. Soc.*, **139**(3), 662 (1992).
2. G. Xu, C. C. Gryte, A. S. Norwick, S. Z. Li, Y. S. Pak, and S. G. Greenbaum, *J. Appl. Phys.*, **66**(11), 5290 (1989).

3. T. C. Farrar, *Introduction to Pulse NMR Spectroscopy,* Farragut Press, Chicago, 1989.
4. A. A. Jones, "Polymer Motion in the Solid State," in *High Resolution NMR Spectroscopy of Synthetic Polymers in Bulk,* R. A. Komoroski, Ed., VCH Publishers, Deerfield Beach, FL, 1986.
5. J. Schaefer, E. O. Stejskal, and R. Buchdahl, *Macromolecules,* **8,** 291 (1975).
6. M. Mehring, *Principles of High Resolution NMR in Solids,* 2nd ed., Springer-Verlag, Berlin, 1983.
7. L. B. Alemany and D. M. Grant, *J. Am. Chem. Soc.,* **105,** 2133 (1983).
8. Oxy Chemical Company literature.
9. G. D. Roberts, D. C. Malarik, and J. O. Robaidek, Viscoelastic Properties of Addition-Cured Polyimides Used in High Temperature Polymer Matrix Composites, NASA TM 103768, 1991.
10. G. Dallas, *Proc. Am. Chem. Soc. Div. Polym. Mat.: Sci. Eng.,* **68,** 336 (1993).
11. S. Li, L. C. Dickenson, and C. W. Chien, *J. Appl. Polym. Sci.,* **43,** 1111 (1991).
12. A. Abragam, *The Principles of Nuclear Magnetism,* Oxford University Press, New York, 1962.
13. T. M. Duncan, *A Compilation of Chemical Shift Anisotropies,* Farragut Press, Chicago, 1990.
14. W. W. Fleming, J. R. Lyerla, and C. S. Yannoni, *ACS Symp. Ser.,* **247,** 83 (1984).
15. L. J. Andrews and R. M. Keefer, *Molecular Complexes in Organic Chemistry,* Holden-Day, San Francisco, 1964.
16. V. M. Svetlichnyi, K. Kalins, V. V. Kudryavtsev, and M. M. Koton, *Doklady Akademii Nauk SSR,* **237,** 612 (1977).
17. F. J. Dinan, W. T. Schwartz, R. A. Wolfe, D. S. Hojnicki, T. St. Clair, and J. R. Pratt, *J. Polym. Sci.: Part A: Polym. Chem.,* **30,** 111 (1992).
18. E. O. Stejskal, J. Schaefer, M. D. Sefcik, and R. A. McKay, *Macromolecules,* **14,** 275 (1981).
19. J. Schaefer, E. O. Stejskal, T. R. Steger, M. D. Sefcik, and R. A. McKay, *Macromolecules,* **13,** 1121 (1980).
20. J. Schaefer, M. D. Sefcik, E. O. Stejskal, and R. A. McKay, *Macromolecules,* **17,** 1118 (1984).
21. A. A. Parker, J. J. Marcinko, Y. T. Shieh, C. Shields, D. P. Hedrick, and W. M. Ritchey, *Polym. Bull.,* **21,** 229 (1989).
22. J. R. Lyerla and C. S. Yannoni, *IBM J. Res. Develop.,* **27,** 302 (1983).

Received September 24, 1993
Accepted January 14, 1994